

Effects of High-Temperature Aging on the Dispersion of Rh/Al₂O₃

DONALD D. BECK AND CONSTANCE J. CARR

Physical Chemistry Department, General Motors Research and Development, 30500 Mound Rd., Box 9055, Warren, Michigan 48090-9055

Received May 24, 1993

The effects of high-temperature treatment in relatively simple gas mixtures of 1% O₂/N₂, 1% H₂/N₂, and an environment which alternates between these two gases on the dispersion of 0.5 wt% Rh/Al₂O₃ were characterized using temperature-programmed desorption (TPD) of D₂. The TPD data was used to determine the relative changes in the Rh metal dispersion as a result of treatment. These treatments were selected as they are believed to model the oxidation and reduction environments in the typical automotive exhaust. When the fresh catalyst was aged in reducing environments at 600, 700, or 800°C, the dispersion decreased rapidly within the first 2 h of treatment, but more slowly thereafter. The rate of this decrease is directly related to the treatment temperature. When the catalyst was aged in oxygen at 600, 700, or 800°C, the Rh was rapidly and completely oxidized. At the lower aging temperatures, most of the Rh could be recovered to the metallic state using a reduction treatment at 200°C, but at 800°C, only a small amount of the Rh was recovered to the metal using this mild reduction treatment. Subsequent reduction treatments at high temperature resulted in near complete recovery of Rh in the form of large metal particles. Treatment in alternating oxygen/hydrogen environments at low frequency produced Rh₂O₃ after each oxidation treatment and Rh metal particles after each reduction treatment. The higher temperature treatments produced sintered Rh metal particles, even in the alternating environment. Treatment in alternating oxygen/hydrogen environments at high frequency resulted in incomplete oxidation of Rh after the oxidation cycle, but did result in more rapid sintering of the Rh metal as the treatment temperature was increased. This sintering rate, however, was slower than for treatments in the pure gases at the same temperature. © 1993 Academic Press, Inc.

INTRODUCTION

The performance of the three-way automotive catalyst (TWC) in the control of CO, NO_x, and hydrocarbon emissions can be affected by operating the catalyst at elevated temperatures (>600°C) (1). A number of changes in the physical characteristics of the catalyst can result from thermal aging, one being the loss of surface area of the catalytically active supported noble metal such as Pt or Rh by sintering (1, 2). A better understanding of this mode of deactivation is needed in order to devise the means for preventing it, and thus improve the durability of the catalyst.

The effects of high-temperature aging on the character of supported Rh are of interest because of the importance of Rh in the catalytic reduction of NO_x (1). The behavior of

supported Rh in a particular environment at elevated temperatures is complicated owing to evidence that, unlike Pt, supported Rh can be easily reduced and/or oxidized under relatively mild conditions (3, 4). Further complication is introduced by evidence that, in the reduced state, supported Rh is believed to exist in several forms including three-dimensional particles, two-dimensional islands, and isolated Rh species (5–8). Supported Rh has been extensively studied by infrared spectroscopy of adsorbate probes such as CO because of the ability to detect and discriminate multi-atom particles, to which CO bonds linearly to an atop site, and small clusters of Rh atoms or even isolated Rh species, to which CO can bond in a gem-dicarbonyl fashion in the presence of Al–OH species (7, 9, 10). Most of these studies have concentrated on the

effects of exposure to reactants such as CO, CO with H₂, or CO with O₂ at moderately high temperatures on the character of the supported Rh. Infrared, XAFS, and TEM evidence suggests that CO itself can disrupt or disperse relatively small Rh particles into isolated Rh(I) species, with the CO bound in a gem-dicarbonyl configuration upon exposure at temperatures below 150°C (8, 10–16). Additional evidence suggests that the presence of hydroxyl groups on the support surface (10, 12, 14, 15) or the presence of NO can assist in the formation of the CO gem-dicarbonyl (17, 18). Exposure to CO at higher temperatures (>200°C) can lead to sintering of the Rh particles (19), although some of the loss of Rh area under extremely high temperature exposure to CO has been attributed to carbon deposition (10).

The sintering of Rh/Al₂O₃ as a result of high temperature treatments (>600°C) in H₂ has also been documented using infrared spectroscopy and chemisorption techniques. Solymosi and Pasztor examined the effect of reduction temperature up to 1000°C on the dispersion of Rh/Al₂O₃ catalyst (13). They found that when the catalyst was reduced at 300 or 400°C, exposure to CO results in the immediate formation of the dicarbonyl species (isolated Rh sites), whereas after reduction at 1000°C, exposure to CO produced mostly linear bonded species (Rh crystallites). Extended exposure to CO in the latter case eventually leads to the creation of isolated Rh atoms. A similar conclusion was reached by Zaki *et al.* (15). Using chemisorption measurements, Fuentes and Figueras (20) were able to obtain low metal dispersions (between 60 and 7.5%) by reducing Rh/Al₂O₃ catalysts at high temperatures (>600°C) for extended periods.

Studies of the effect of high-temperature treatments in an oxidizing environment on the character of Rh/Al₂O₃ have resulted in conflicting observations. For instance, using electron microscopy and anomalous X-ray diffraction, Yates and Prestridge found when Rh/Al₂O₃ was calcined at 650°C, a metal dispersion of 48% was obtained, but

when the catalyst was calcined at 760°C, a much lower metal dispersion of 6.3% was measured (21). On the basis of similarly treated catalysts which were subsequently analyzed using electron microscopy (22), the authors suggested that the low dispersion value obtained after the higher temperature oxidation was explained by the formation of large (500–1000 Å) platelets of Rh₂O₃. In an additional experiment, a sample was calcined at 760°C, reduced at 500°, passivated at room temperature, and examined using TEM. Particles of Rh were observed with diameters <300 Å, but yielded no Rh diffraction lines. The authors suggested on the basis of these observations that metallic Rh islands were formed by reduction of the Rh₂O₃ platelets. Other researchers have suggested that in the transfer of a reduced Rh/Al₂O₃ catalyst to the TEM, exposure to air compromised the state of the supported metal after reduction (11). In a separate study, however, Yao *et al.* suggested that when Rh/Al₂O₃ was oxidized at temperatures above 600°C, an oxide of Rh forms and diffuses into the bulk of the Al₂O₃ (23). In that work, the authors also claimed that the process could be only partially reversed by subsequent reduction at similar temperatures (>550°C). The behavior of Rh/Al₂O₃ at high temperatures (>600°C), particularly in an oxidizing medium, is apparently not well understood and warrants additional study.

In this work, the effect of aging at high temperature (between 600 and 900°C) on the character of a Rh/Al₂O₃ catalyst was characterized using temperature programmed desorption (TPD) of D₂ in an ultrahigh vacuum instrument. In a previous report, the authors employed the same technique to characterize the sintering kinetics of Pt/Al₂O₃ as a function of aging time and environment and were able to detect rapid changes in the character of the supported metal induced by thermal aging (24). In this work, an apparatus was used which allowed the sample to be treated in a high-pressure cell at high temperatures (up to 900°C) in the flowing gas

at atmospheric pressure, and then directly transferred to a vacuum chamber and characterized using TPD of D_2 .

EXPERIMENTAL

Materials

A 0.5 wt% Rh/ Al_2O_3 catalyst used in this study was prepared in the following manner. A 100-g portion of W. R. Grace low bulk density alumina spheres was treated with a solution of 1.501 g $[Rh(NH_3)_6]Cl_3$ in 100 ml of water. This lot of catalyst was air-dried overnight in a hood and then calcined in flowing air at 460 standard cm^3/min (SCCM) for 2 h at 500°C. A portion of this catalyst was ground and sieved using a 100-mesh sieve for the experiments conducted in this study. The dispersion of this catalyst as measured using the chemisorption of H_2 (25) was found to be 63%. Alumina powder used for blank experiments was obtained from the same lot of alumina spheres before impregnation with the metal. The gases used in this study were obtained from Scott Specialty Gases and included 1% O_2/N_2 , 1% H_2/N_2 , and D_2 (99.7% CP grade), the latter being purified by passage through a liquid-nitrogen trap before use.

Apparatus

The experiments were performed in an ultrahigh vacuum system (base pressure 5×10^{-10} Torr, working pressure 5×10^{-9} Torr (mostly H_2O)) equipped with a mass spectrometer, a hemispherical electron energy analyzer, two differentially pumped ion guns, an electron gun, and an X-ray source. A small-volume (10 cc) high-pressure chamber is attached to the vacuum system and is isolated from the vacuum chamber and ambient by a series of spring-loaded Teflon seals. The volume between each set of seals is differentially pumped to below 1×10^{-8} Torr. The high-pressure chamber was used for sample preparation and gas dosing, while the vacuum chamber was used for sample analysis using temperature programmed desorption (TPD). The sample was mounted on a 20-mm-o.d. sample transfer manipula-

tor capable of linear and rotary motion through the seals. Because the sample is loaded in a sealed cutout section some distance from the end of the manipulator, the two chambers remain isolated with respect to each other and with respect to ambient air regardless of the sample position. The primary advantage of this instrument in the study of catalysts is that samples can be treated in the preparation chamber and then transferred to the analysis chamber for characterization without exposing the sample to air, thus protecting the character of air-sensitive samples.

The sample boat is constructed from an iron-chromium-aluminum-rare earth alloy foil obtained from Allegheny Ludlum (26). A $10 \times 10 \times 1.0$ -mm section of this foil was treated in air at 1100°C for 8 h to create an alumina film on the surface. The film consists entirely of α -alumina and has a spongy morphology. One side of this section of foil was cleaned to remove the alumina layer and spot-welded to two support foils of the same material. The support foils were mounted on two copper blocks, each being brazed to the end of an electrical current vacuum feedthrough. Sample heating was accomplished by applying electrical current across the sample holder.

Using this heating method, the sample was heated routinely to a maximum of 1000°C in vacuum and 900°C in 760 Torr of 1% O_2/N_2 flowing at 10 SCCM. The ability to uniformly heat a sample was important for TPD experiments and was tested in the following way. During a TPD experiment, the temperature was simultaneously measured at five different locations on the oxidized portion of the sample holder using chromel-alumel thermocouple junctions. Four of the junctions were attached near the corners of the sample holder, while the remaining junction was attached near the center. When temperature of the sample holder was increased linearly in the vacuum chamber, the temperature gradient across these points did not exceed 3°C. When the sample holder was heated to 800°C in 760

Torr of 1% O₂/N₂ flowing at 10 SCCM, the temperature gradient across the sample did not exceed 6°C. In subsequent experiments, the sample temperature was obtained using a single thermocouple attached near the center of the oxidized foil. Catalyst powder samples were slurried with distilled water and coated on the center of the alumina film surface. After it was dried at 25°C in air, the sample was transferred to the pretreatment chamber for experimentation. After completion of an experiment, the sample was removed and weighed.

Samples were treated in the high-pressure chamber in two ways. For controlled dosing experiments at pressures less than 1 Torr, either D₂ or CO gas was admitted to the chamber through a leak valve. For controlled atmosphere aging treatments, the following procedure was used. The gate valve between the chamber and the turbomolecular pump was closed and either 1% O₂/N₂ or 1% H₂/N₂ was admitted to the chamber at 760 Torr and a flow rate of 10 SCCM through a mass flow controller and a bellows valve. After flowing through the chamber the gas is allowed to exit via a bellows valve. During the aging treatments, the chamber walls were cooled by circulating chilled water (15°C) through coils which are in contact with the outside of the chamber. With no gas admission to the chamber, the base pressure was typically 1×10^{-8} Torr after bakeout, and typical working pressure was below 5×10^{-8} Torr.

Initial Catalyst Pretreatment

Catalyst samples were initially pretreated by placing the sample in the high-pressure chamber and exposing them to a flow of 1% O₂/N₂ at 10 SCCM. The sample temperature was slowly increased at a rate of 5°C/min to 500°C, remaining at 500°C for 30 min. At the end of this treatment, the sample was then allowed to cool to 25°C, and then the flowing gas composition was changed to 1% H₂/N₂ flowing at 10 SCCM. The sample was again heated at a rate of 5°C/min to 500°C, remaining at that level for 30 min, and then

finally cooled to 25°C. This sample "cleaning" procedure was adopted in order to obtain a "stable" fresh catalyst dispersion using TPD measurements.

Aging Treatments

Catalyst samples were aged in the high pressure treatment chamber using the following method. After pretreatment, the sample was exposed to the treatment gas (either 1% H₂/N₂ or 1% O₂/N₂) in flowing at 10 SCCM at 25°C. The temperature of the sample was then rapidly increased to a chosen value, remaining at that value for a chosen length of time, and then rapidly cooled to near 25°C. The sample was then moved to the analysis chamber and flash-heated in the vacuum environment to 500°C, followed by cooling to 25°C to remove part of the adsorbed H₂O and all of the adsorbed H₂. When aging treatments in 1% O₂/N₂ were performed, a subsequent treatment in 1% H₂/N₂ was carried out at 200°C for a period of 10 min to reduce the Rh₂O₃ formed during oxidation to Rh metal. This mild reduction treatment was chosen since it has been found to be sufficient to reduce small unsupported Rh₂O₃ particles to Rh metal (3). Each aging treatment was followed by a series of TPD experiments. Treatments at a chosen temperature were repeated until an accumulated aging time of 4 h was obtained.

For some experiments, alternating treatments in 1% O₂/N₂ and 1% H₂/N₂ were used to simulate a "cycled" aging environment. After each treatment in the oxidizing environment in this series of experiments, the sample was given a brief reduction treatment at 200°C before performing the TPD analysis.

Temperature-Programmed Desorption Measurements

TPD experiments were conducted using the following procedure. The sample was exposed to D₂ at 10 Torr for a chosen length of time in the pretreatment chamber. During this exposure, the gate valve was open to the turbomolecular pump. At the end of the

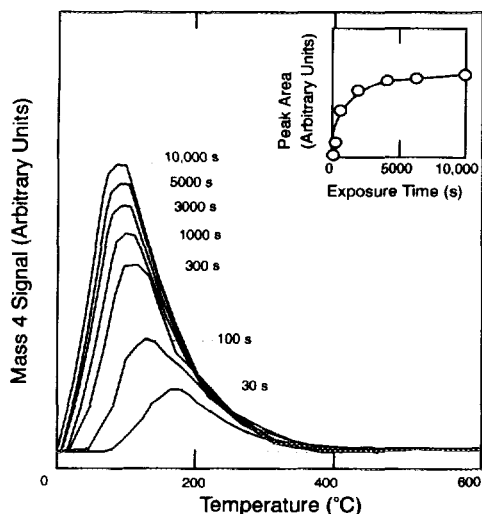


FIG. 1. D_2 TPD from 0.5% Rh/ Al_2O_3 for various dose times at 10 Torr. Inset: Area of TPD peak as a function of dose.

exposure, the sample was transferred to a position facing the inlet of the mass spectrometer in the analysis chamber. A TPD spectrum was then obtained by heating the sample at linear rate of $4^\circ\text{C}/\text{s}$. During the heating program, the partial pressures of D_2 and other relevant desorbing gases were measured as a function of time (and temperature) using the mass spectrometer, which was interfaced to an AST 80486-based personal computer.

The following procedure was carried out to determine a minimum dose length necessary to obtain a near saturation coverage of adsorbate for the TPD experiment. A fresh sample of the 0.5 wt% Rh/ Al_2O_3 catalyst was pretreated using the procedure described earlier. A series of TPD experiments were performed in which the exposure of the sample at 40°C to 10 Torr of D_2 was varied between 10 and 10,000 s. Selected TPD spectra are shown in Fig. 1. All display a single peak having a maximum intensity (T_p) at 100°C . The peak area (inset of Fig. 1) increased rapidly as a function of increasing dose time, but then increases gradually after a dose time of about 100 s. In subsequent TPD ex-

periments involving D_2 , exposure at 10 Torr for 1000 s was used to create a near saturation adsorbate coverage.

Similar experiments were carried out using a blank alumina sample pretreated in the same fashion. The results, shown in the dashed line in Fig. 1, indicates that adsorption on the support alone is insignificant relative to adsorption on the Rh-containing sample. No detectable signal was observed from the sample holder alone, which was also examined using D_2 TPD. This comparison suggests that the single peak observed when the experiment is performed using the Rh/ Al_2O_3 sample can be attributed almost entirely to deuterium adsorbed on Rh metal surfaces.

Measurements of the Rh surface area as a function of aging in reducing environments were repeated using multipoint chemisorption of H_2 using a Micromeretics Chemisorb 2800 instrument. For this series of experiments, aging treatments were also performed *in situ* and interrupted periodically in order to obtain a dispersion measurement. A more detailed description of the measurement procedure using this instrument has been discussed elsewhere (25).

RESULTS AND DISCUSSION

TPD of D_2 on Rh/ Al_2O_3

We have demonstrated in a previous study (24) that the area of the TPD peak attributed to adsorption on Pt can be taken as a relative measure of the noble metal surface area, given that at saturation coverage, D/M_s maintains a constant stoichiometry. In studies of adsorption of H_2 on single-crystal Rh surfaces, the H/M_s ratio is near unity at saturation coverage (27–29). Using chemisorption and TEM measurements, other researchers have concluded that for relatively large supported Rh particles ($d > 4$ nm), the H/M_s ratio is near unity (20, 21, 30, 31). However, the assignment of a constant stoichiometry is difficult for highly dispersed supported Rh (31). For instance, other researchers have reported H/M values exceeding unity in the study of ultradispersed

Rh using H₂ chemisorption (32, 33). These results can be explained by an incorrect accounting of the reversible part of the adsorption (25), hydrogen spillover (25, 34), accommodation of hydrogen in the subsurface region of particles (35, 36), and increased H/M stoichiometry due to multiple adsorption on sites of low metal coordination (37, 38). The H/M ratio, however, probably remains near unity for catalysts of moderate to low dispersion.

Although CO TPD can also be used to gain additional insight to the determination of Rh surface area and indeed to the distribution of highly dispersed Rh atoms or clusters vs larger Rh particles, it was considered to be less useful because of the greater uncertainty in CO/M. For adsorption of CO on supported Rh, multiple binding states are possible including gem-dicarbonyl bonding on isolated Rh atoms or clusters, as well as linear and bridge-bonding on Rh particles, all of these cases having been well documented. We have found that several binding states between CO and Rh metal can be identified in the TPD spectrum, but these states are difficult to resolve when Rh supported on a high surface area alumina is studied. Certainly, performing a simultaneous infrared measurement would assist in better identification of these states. Until more complete TPD studies have been reported, quantitative infrared adsorption remains better suited as a technique to measure the Rh surface area using CO adsorption, as demonstrated by Rasband and Hecker (39).

Initial experiments using supported Rh catalysts were difficult to characterize using TPD due to the high degree of irreproducibility in the TPD spectral areas. Thus, the following series of experiments were performed using both fresh and aged Rh/Al₂O₃ catalyst samples (aging treatment at 600°C for one h in 1% H₂/N₂) in order to obtain reproducible TPD results. In the first series of experiments, a pretreated but unaged Rh/Al₂O₃ sample was characterized by performing D₂ TPD experiments until the spec-

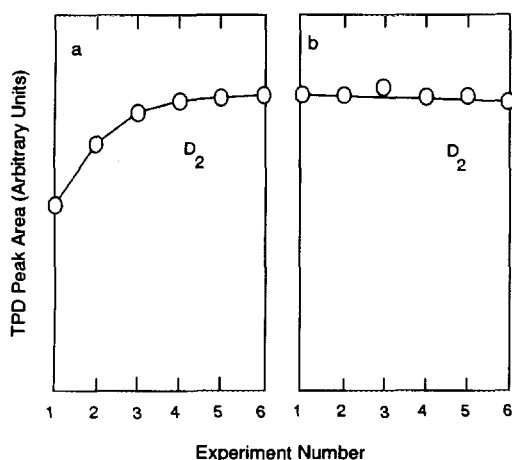


FIG. 2. (a) Change in the D₂ TPD peaks as the TPD measurements are repeated. A fresh catalyst was used for each TPD experiment. (b) Change in the D₂ TPD peaks as the measurements were repeated, this time after pretreatment of the catalyst in 1% H₂/N₂ at 600°C for 1 h.

tral shape and area were reproducible. The resulting TPD areas for these experiments are shown in Fig. 2a as a function of the order in the sequence. Note that at the beginning of the sequence, the D₂ TPD area is relatively low. As the experiment was repeated, the D₂ area increases. Eventually, the D₂ TPD area could be reproduced. Therefore, in all subsequent measurements involving the fresh Rh/Al₂O₃ catalyst, the TPD procedure was repeated until the spectra were reproducible. The TPD areas were then taken to be representative of the "stable" fresh catalyst. In the second series of experiments, a fresh Rh/Al₂O₃ sample was pretreated, then aged at 600°C in 1% H₂/N₂ flowing at 10 SCCM for 1 h. Consequent D₂ TPD experiments were performed and were found to be easily reproducible (Fig. 2b). In practice, the authors found that when the catalyst was aged in more severe environments, subsequent TPD measurements were also repeatable.

The authors note that other investigators have found that adsorbed water can greatly affect H₂ TPD measurements (38). Furthermore, heating to 500°C in vacuum only par-

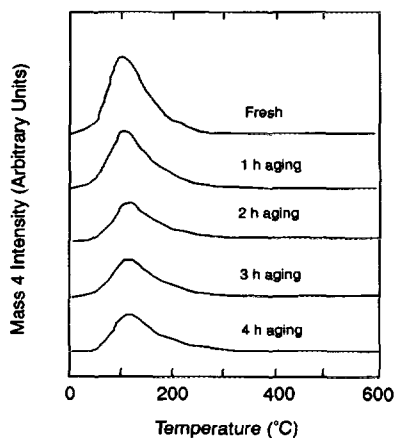


FIG. 3. TPD of D_2 after 1 h aging treatments in 1% H_2/N_2 at $800^\circ C$.

tially removes surface hydroxyl groups (40). Thus, we suggest that the initial irreproducibility in the TPD spectra can be attributed to the influence of surface hydroxyl groups, which are removed in the initial TPD experiments. When most of the influential surface hydroxyl groups have been removed, reproducible TPD spectra can then be obtained. The detection of an HDO peak in the TPD which decreases in intensity as the experiments with the fresh catalyst are repeated suggests that D_2 can initially react with surface hydroxyl groups to form water, but after several TPD experiments, the a sufficient number of surface hydroxyl groups have been removed by reaction and desorption such that the influence of remaining species on subsequent adsorption of D_2 is no longer significant.

Although the catalyst was heated to $600^\circ C$ toward the end of each TPD experiment, the sample was immediately cooled at the end of the temperature program to minimize the impact of thermal treatment in vacuum on the dispersion of the catalyst. Although we recognize that some sintering of the Rh is possible during a TPD experiment, the observation that the D_2 TPD area increases as the experiment is repeated suggests that any sintering during the procedure used here is relatively insignificant.

Aging in 1% H_2/N_2 at High Temperatures

The influence of thermal aging in a reducing environment on the Rh/Al_2O_3 catalyst was investigated by performing the following experiments. A fresh Rh/Al_2O_3 catalyst was pretreated according to the procedure described earlier and characterized using D_2 TPD (Fig. 3). The sample was then aged in 1% H_2/N_2 at $800^\circ C$ for 1 h, and then characterized again using D_2 TPD (Fig. 3). This procedure was repeated until an accumulated aging time of 4 h was reached. Upon aging for several 1-h intervals, the D_2 TPD peak area increased to a maximum, then decreased gradually. The D_2 TPD peak shape did not change significantly as a result of successive aging treatments.

This procedure was repeated for all treatment temperatures (600 , 700 , and $800^\circ C$). In each of these experiments, treatment intervals of 20 min or longer were used until a sum of 4 h was obtained. At the end of each treatment interval, the apparent dispersion was estimated from the D_2 TPD peak area. The change in the apparent dispersion determined from D_2 TPD as a function of aging time for all three aging temperatures is shown in Fig. 4. The apparent dispersion

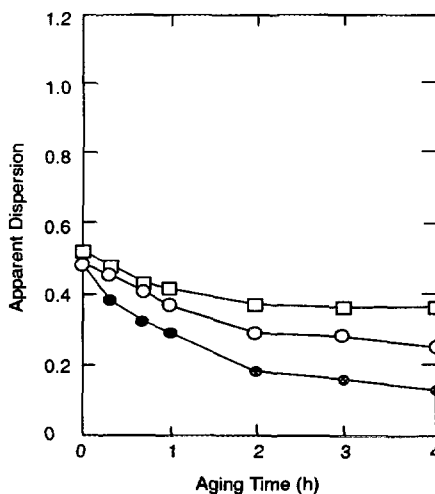


FIG. 4. Apparent dispersion determined from the D_2 peak versus aging time in 1% H_2/N_2 for various aging temperatures: (\square) $600^\circ C$, (\circ) $700^\circ C$, and (\bullet) $800^\circ C$.

TABLE I
Apparent Dispersion of 0.5 wt% Rh/Al₂O₃ as a
Function of Aging in 1% H₂/N₂

Aging time (h)	Temperature (°C)		
	600	700	800
0(fresh)	0.52(0.59) ^a	0.55(0.61)	0.53(0.62)
1	0.43(0.46)	0.39(0.41)	0.34(0.36)
2	0.35(0.40)	0.27(0.31)	0.19(0.21)
3	0.34(0.36)	0.28(0.30)	0.15(0.16)
4	0.32(0.35)	0.23(0.25)	0.14(0.15)

^a Value obtained using D₂ TPD. Value in parentheses obtained using chemisorption of H₂.

values obtained at 1-h aging intervals using D₂ TPD are listed in Table I for all three treatment temperatures, as well as the corresponding results obtained from the chemisorption experiments. Note the general agreement between the TPD results and the chemisorption measurements. This agreement suggests that the H/M ratio indeed remains relatively constant over the course of the aging treatments, which is partly attributable to the fact that the beginning dispersion of 0.5–0.6 is indicative of moderately (not highly) dispersed Rh particles. This agreement also confirms that TPD can be used to reliably determine Rh surface area if the adsorption of the probe molecules is not inhibited, as we have discussed in the previous section. The observation of an initial increase in the apparent dispersion during aging treatments at 600°C can also be attributed to an initial inhibition of D₂ adsorption by residual hydroxyl groups as we will suggest in the following section. Although this initial increase in dispersion was not repeatedly detected in the chemisorption measurements, it was duplicated in the TPD experiments.

We note the dispersion measured using conventional H₂ chemisorption (60%) and by D₂ TPD (50–55%) implies a mean particle size of ~2.0 nm; thus, an assignment of D/Rh = 1 for the existing Rh particles is reasonable. Since the Rh particles exist as

a distribution of particle sizes, some of the Rh may exist in the form of very small clusters or isolated atoms. The true distribution of Rh particle size is typically difficult to determine in these catalysts since the particles are difficult to detect even using high resolution transmission electron microscopy. It is unlikely that adsorption of D₂ on isolated Rh or small metal clusters is inhibited or occurs by an activated process since many researchers have observed extremely high H/M stoichiometries for ultra-dispersed Rh catalysts. Rather, we believe that the observation of an initial increase in the D₂ TPD area at the lowest aging temperature (600°C) is attributable to the further removal of hydroxyl groups, resulting in even less inhibition of D₂ adsorption on the Rh surfaces. This would explain the initial increase in the D₂ TPD area with aging, followed by a subsequent decrease with longer aging treatment, the latter observation being consistent with the sintering of the Rh particles being dominant. At present we believe that this effect was not observed in the chemisorption measurements due to the longer evacuation times at elevated temperatures used in the latter.

Note also that the initial rate of sintering for the highly dispersed Rh moieties increases with increasing aging temperature. At higher aging temperatures, the initial increase in the D₂ TPD probably occurs too rapidly to be observed using treatment intervals of 10 min. We also observed that the relative rate of sintering for these particles is dramatically lower than that observed in a 1 wt% Pt/Al₂O₃ catalyst aged under the same conditions (24), confirming the relative resistance of Rh to sintering in these environments.

Some insight about the dominant sintering mechanism may be gained by fitting the sintering data to a simple model. One of these models has been developed on the basis of particle migration/agglomeration. Such a model takes the form of a power law function such as $(n) \log(D_0/D_t) = \log t + C$, where D_0 is the initial dispersion, D_t is the

dispersion at time t , C is a constant, and n is the sintering order (24). An alternative model, which has been developed on the physical basis that sintering takes place by the transfer of metal atoms from small particles to larger ones, in its simplest form takes a function such as $-dD/dt = kD^n \exp(mD)$, where k is the sintering rate constant, m is a factor dependent on particle morphology, metal-vapor interfacial energy, metal-support contact angle, and temperature (m is generally a constant at constant temperature), and n is a constant dependant on the mode of transport (24).

Our results were fit according to the former model and plotted as $\log D_0/D_t$ vs \log aging time (see Fig. 6). Due to the scatter in the data, it is difficult to determine whether the results conform to a linear function or a nonlinear function which gradually decreases in slope with increasing aging time. The best linear fit to the data produced relatively low sintering orders between 4.7 and 1.6. As we have discussed in a previously reported study (24), the observation of relatively low sintering orders has been associated with a sintering mechanism which is dominated by atom transport from small particles to larger ones. This is consistent with suggestions that the interaction between Rh and alumina is relatively strong and would inhibit particle migration.

Aging in 1% O₂/N₂ at High Temperatures

The effects of an oxidizing chemical environment on the Rh/Al₂O₃ catalyst are expected to be quite different from a reducing environment. To investigate these effects, thermal aging of the 0.5 wt% Rh/Al₂O₃ catalyst in 1% O₂/N₂ was investigated by performing the following experiments.

Measurement of the available Rh surface area and subsequent determination of dispersion were obtained using D₂ TPD measurements taken at 1-h intervals as a function of sintering time in 1% O₂/N₂ until an accumulated aging time of 4 h was obtained. After the first oxidation treatment, complete oxidation of the supported Rh was indicated

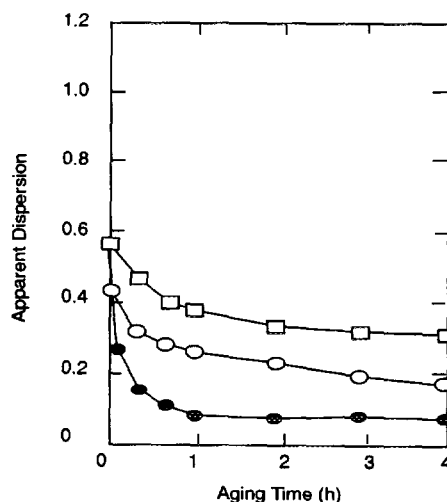


FIG. 5. Apparent dispersion determined from the D₂ peak versus aging time in 1% O₂/N₂ for various aging temperatures. (Each high-temperature treatment was followed by a mild reduction treatment at 200°C for 10 min.) Symbols are as in Fig. 4.

by the absence of any signal in the subsequent D₂ TPD. Therefore, after each high-temperature treatment in 1% O₂/N₂, the catalyst was given a "mild" reduction treatment in 1% H₂/N₂ at 200°C prior to analysis using TPD which is expected to completely reduce surface Rh₂O₃. Subsequent aging treatments at 800°C do not result in significant further changes in the shape or area of the D₂ TPD spectra.

This procedure was repeated for all three treatment temperatures (600, 700, and 800°C). In each of these experiments, treatment intervals of 20 min or longer were used until a total accumulated aging time of 4 h was obtained. The change in the apparent dispersion determined from D₂ TPD as a function of aging time for all three aging temperatures are shown in Fig. 5. The apparent dispersion values obtained at one h aging intervals using D₂ TPD are listed in Table 2 for all three treatment temperatures. Several trends are notable in the data. First, we note that the magnitude of the decrease after several hours of treatment is dependent on the aging temperature, as is the case

TABLE 2
Apparent Dispersion of 0.5 wt% Rh/Al₂O₃ as a
Function of Aging in 1% O₂/N₂

Aging time (h)	Temperature (°C)		
	600	700	800
0(fresh)	0.49 ^a	0.52	0.55
1	0.37	0.24	0.07
2	0.31	0.22	0.06
3	0.30	0.16	0.07
4	0.29	0.16	0.06

^a Value obtained using D₂ TPD.

in 1% H₂/N₂. Note that the apparent dispersion decreases rapidly at the highest aging temperature and reaches a plateau within a single hour of treatment. At the lower aging temperatures, the initial rate of decrease in the apparent dispersion is greater than at the equivalent aging temperature in H₂, but does not reach a plateau over the 4 h aging period.

A comparison between oxygen-aging and hydrogen-aging suggests the decrease of Rh surface area is more rapid in the oxidizing environment at 600 and 700°C. However, a much greater contrast in the comparison is observed at a treatment temperature of 800°C. In this case, almost all of the exposed Rh disappears within a short period (20 min) when the sample is aged in 1% O₂/N₂. Our TPD results suggest that oxidation at high temperature (>700°C) followed by reduction at low temperature (200°C) appears to sinter the supported metal more effectively than a reduction treatment alone at the same temperature (>700°C). However, additional observations discussed in the next section will show that indeed after oxidation at high temperature (>700°C), not all of the Rh is reduced to the metallic form by reduction at 200°C.

As a final note, these results were plotted in Fig. 6 as log(D₀/D_t) vs log aging time to determine whether they fit the power law relationship. For all aging temperatures, the

linearity of the data in the region between 1 and 4 h could not be distinguished due to the scatter. The best linear fits to the data resulted in relatively low sintering orders for aging at 700 and 600°C, but the sintering order was found to be relatively high ($n \sim 9$) for aging at 800°C. The latter value for n is suggestive of a sintering mechanism dominated by particle migration.

Cycled Aging at High Temperature and Low Cycling Frequency

In practice, an automotive catalytic converter is subjected to an exhaust gas feed-stream that oscillates between a "rich" (reducing) mixture and a "lean" (oxidizing) mixture (41, 42). The frequency of this oscillation is generally on the order of 0.5 to 1 Hz. The effects of this "cycled" aging schedule on the properties of the catalyst are of interest to study. Therefore, in the following experiments, the 0.5 wt% Rh/Al₂O₃ catalyst was exposed to alternating treatments in 1% O₂/N₂ and in 1% H₂/N₂ at

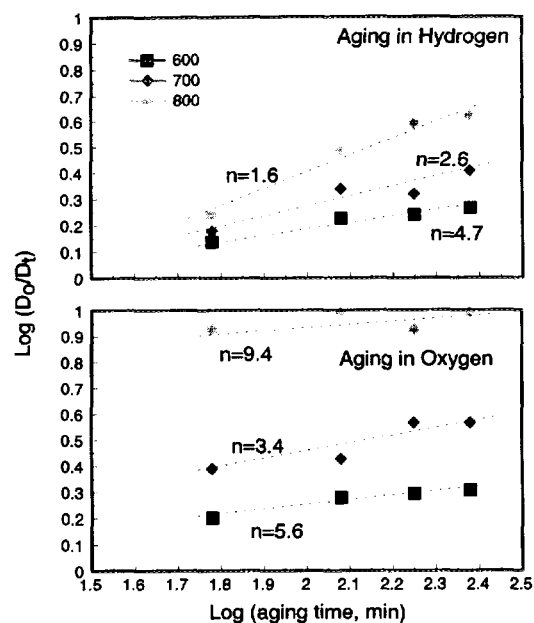


FIG. 6. Plot of log D₀/D_t vs log t for various aging temperatures in 1% H₂/N₂ (upper graph) and in 1% O₂/N₂ (lower graph).

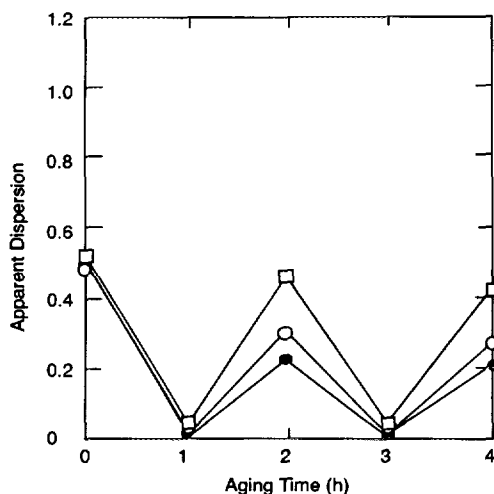


FIG. 7. Apparent dispersion determined from the D_2 peak versus treatment alternating between 1% O_2/N_2 and 1% H_2/N_2 for various aging temperatures. Each high temperature treatment was 1 h in duration. Cycled aging: 0.00014 Hz. Symbols are as in Fig. 4.

a chosen temperature. Treatments in each environment were carried out using one of two durations: 1 h (slow oscillation at 0.00014 Hz) and 5 s (fast oscillation at 0.1 Hz). The slow oscillation was performed to simulate an extreme in lack of closed-loop control in the exhaust, while the fast oscillation was performed to simulate closed-loop operation. Although in actual vehicle exhaust, closed-loop operation cycles on a time scale closer to 1 Hz, treatments were performed at a minimum of 5 s due to limitations in the present apparatus.

After pretreatment, a sample was characterized using D_2 TPD and was then aged in 1% O_2/N_2 for a selected time and temperature. Characterization using D_2 TPD was repeated, followed by aging the sample in 1% H_2/N_2 for the same time period and temperature, followed by another characterization by D_2 TPD. The sample was thus exposed to alternating environments and characterized by TPD after each treatment until a total treatment time of 4 h was reached. For treatments of 1 h in each environment, two sets of experiments were car-

ried out: for the first set, treatments simply alternated between 1% O_2/N_2 and 1% H_2/N_2 at high temperature, while for the second set, each treatment in 1% O_2/N_2 was followed by a mild reduction treatment in 1% H_2/N_2 at 200°C for 10 min. For treatments of 5 s, D_2 TPD experiments were carried out only after total treatment times of 1 h.

The change in the apparent dispersion determined from D_2 TPD as a function of treatment sequences for all three treatment temperatures are shown in Fig. 7 for treatments of 1 h duration in each environment. The apparent dispersion values obtained using D_2 TPD are also listed in Table 3 for these experiments. The results are straightforward in that no metal surface can be measured after each oxidation treatment, indicating that the Rh is completely oxidized and is not able to chemisorb D_2 at ambient temperature. The metal surface area is easily recovered by subsequent treatment in 1% H_2/N_2 at 600°C, but recovery is only partial after treatment at the higher temperatures.

The experimental series was repeated, except that the catalyst sample was exposed

TABLE 3

Apparent Dispersion of 0.5 wt% Rh/ Al_2O_3 as a Function of Aging in Alternating 1% O_2/N_2 and 1% H_2/N_2 Treatments (Alternation at 1 h Each Treatment)

Aging treatment	Temperature (°C)		
	600	700	800
0(fresh)	0.52 ^a	0.53	0.55
1(oxidation)	0.02	0.01	0.02
2(reduction)	0.47	0.32	0.25
3(oxidation)	0.03	0.02	0.03
4(reduction)	0.38	0.30	0.23
(Each oxidation at high temperature followed by reduction at 200°C for 10 min)			
0(fresh)	0.52 ^a	0.53	0.55
1(oxidation)	0.35	0.21	0.07
2(reduction)	0.48	0.32	0.25
3(oxidation)	0.31	0.16	0.06
4(reduction)	0.39	0.30	0.22

^a Value obtained using D_2 TPD.

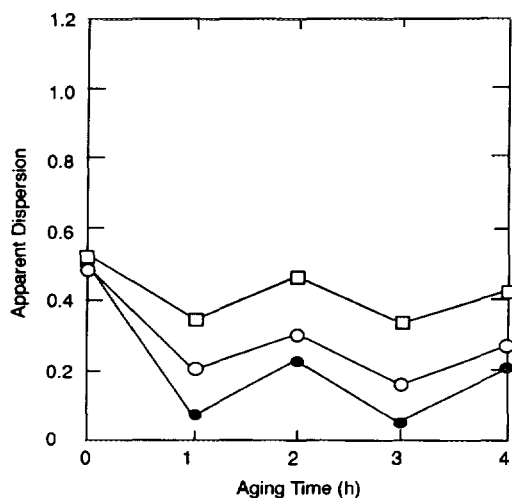


FIG. 8. Apparent dispersion determined from D₂ peak versus treatment alternating between 1% O₂/N₂ and 1% H₂/N₂ for various aging temperatures. Each treatment was 1 h in duration. In this case, each high-temperature treatment was 1 h in duration. In this case, each high-temperature oxidation treatment was followed by a mild reduction treatment at 200°C for 10 min prior to characterization by TPD.

to a mild reduction treatment at 200°C for 10 min after each high-temperature oxidation and prior to the high-temperature reduction in the series. The apparent dispersion determined from D₂ TPD as a function of treatment sequence for all three treatment temperatures in these experiments are shown in Fig. 8. It is of interest to note that the high temperature reduction treatment recovers a greater amount of the Rh metal surface area than the mild reduction treatment at 200°C. This effect was more dominant at 700 and 800°C. Note also that after the first cycled treatment at all treatment temperatures, the total Rh metal surface area recovered in subsequent cycled treatments continues to decrease slightly at 600°C and more significantly at 700 and 800°C. For a particular aging temperature, the measured Rh surface area after four 1-h cycled treatments was higher than that after 4 h (or even 2 h) in the reducing environment, and significantly higher than that after 2 h in the oxidizing environment. The total

Rh surface area was never completely recovered as a result of aging in a cycled environment at 700 or 800°C, and a significant portion was lost at 800°C.

The behavior of the measurable Rh surface area after each stage of the cycled aging experiment demonstrates the reversible oxidation–reduction property of supported Rh, in agreement with previously reported work (43). The observation that after severe oxidation at 700 or 800°C, more Rh surface area was recovered by subsequent reduction at 700 or 800°C, respectively, than at 200°C indicates that as a consequence of the oxidation treatment, a large portion of the Rh was converted into a reduction-resistant species. These moieties do not exist in the form of surface Rh₂O₃ crystallites, since even bulk Rh₂O₃ can be completely reduced near 200°C (3). A more reasonable explanation is a strong interaction with the support which has been activated by the high-temperature oxidation treatment, explained by some as the formation of a spinel with alumina (23). The X-ray diffraction spectrum of the Rh/Al₂O₃ catalyst obtained after oxidation at 800°C provides no evidence for a Rh oxide crystal structure or formation of a compound with Al₂O₃. However, such a compound may escape detection due to the low concentration in the support, insufficient crystallite domain size, or distorted lattice. Whatever the form of this species, reduction at high temperature returns (1) at least a portion of the “lost” Rh to the surface of Al₂O₃, or (2) all of the “lost” Rh to the surface, but in a sintered form.

The portion of Rh that is reduced at 200°C following the oxidation treatment at 700 or 800°C is attributed to that part of the Rh which forms Rh₂O₃ crystallites and remains on the surface during the oxidation treatment and which is later reduced to Rh particles during the mild reduction treatment. Our observations suggest that after oxidation at the highest temperature (800°C), only a minor amount of the Rh remains on the surface to form Rh₂O₃ crystallites, while at the lowest treatment temperature (600°C),

most of the Rh remains on the Al_2O_3 surface in the oxide form. The Rh metal surface area measured after each reduction phase continues to decrease slightly in the cycled treatments at 600°C , and more significantly in the cycled treatments at 700°C . However, after the first cycled treatment at 800°C , the Rh metal surface area is completely recovered in subsequent cycled treatments. Since the thermal damage imparted to the catalyst as a result of aging in a cycled oxidation/reduction environment is slightly less than that in a reducing environment at the same temperature, the cycled aging environment appears to provide support for maintaining dispersion of Rh particles, but not highly dispersed Rh atoms or clusters. These observations suggest that, as a result of cycled treatments at the higher temperatures, isolated Rh atoms eventually migrate close to a particle. In a reducing environment, these Rh species can coalesce to form a particle. In oxidizing conditions, this Rh converts to the oxide phase, but remains in close proximity where it will form a particle again upon reduction.

Cycled Aging at High Temperature and High Cycling Frequency

Treatments in alternating gas environments were also performed using a faster cycling frequency of 0.1 Hz. These cycling treatments were halted at 1-h intervals for characterization by D_2 TPD. After the first 1 h of treatment, the sample was characterized two times: at the end of the 5-s oxidizing treatment (filled symbols) and at the end of the subsequent 5-s reducing treatment (open symbols). This procedure was repeated at the end of each 1 h of treatment until a cumulative total of 4 h was reached. The results, shown in Fig. 9 and listed in Table 4, indicate that at the lower treatment temperatures, the Rh metal particles do not completely oxidize at the end of each exposure to oxygen, and that during exposure to this cycled environment, gradual sintering does occur, but is less rapid than for treatment in a single gas at the same temperature. At the higher

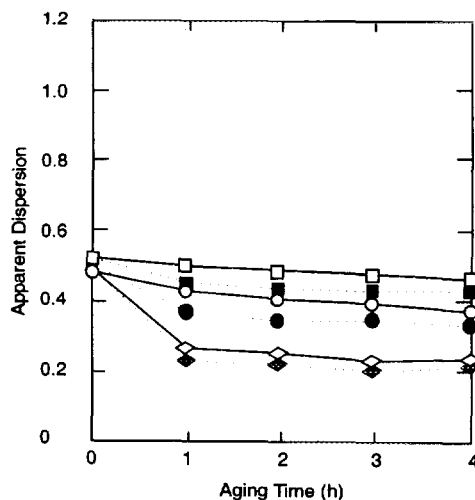


FIG. 9. Apparent dispersion determined from the D_2 peak versus treatment alternating between 1% O_2/N_2 and 1% H_2/N_2 for various aging temperatures. Each treatment was 5 s in duration. Open symbols represent reducing treatment and filled symbols represent oxidizing treatment. (□, ■) 600°C , (○, ●) 700°C , and (◇, ◆) 800°C . Cycled aging: 0.1 Hz.

treatment temperatures, some oxidation of the Rh particles is noted after each exposure to oxygen early in the treatment schedule, but as the particles become larger through sintering, the oxygen treatments have a smaller effect: the Rh particles remain mostly in the metallic state. Only partial oxidation of the Rh particles, if any, occurs. These experiments comment on the effect of cycling frequency on the catalyst character and suggest that Rh metal particles, and consequently catalyst activity, are better preserved in the metallic state by increasing the cycling frequency during exposure to alternating oxidizing/reducing environments. Although these experiments also suggest that higher cycling frequencies result in an initially slower Rh metal particle sintering rate, they do not predict the character of the supported metals over exposures much greater than 4 h (see Table 4).

In summary, the character of a 0.5 wt% Rh/ Al_2O_3 catalyst has been studied as a function of treatment in reducing, oxidizing, and cycled environments at relatively high

TABLE 4

Apparent Dispersion of 0.5 wt% Rh/Al₂O₃ as a Function of Aging in Alternating 1% O₂/N₂ and 1% H₂/N₂ Treatments (Alternation at 5 s Each Treatment)

Aging treatment	Temperature (°C)		
	600	700	800
0(fresh)	0.53 ^a	0.51	0.48
1(oxidation)	0.44	0.38	0.22
1(reduction)	0.49	0.42	0.26
2(oxidation)	0.43	0.35	0.21
2(reduction)	0.47	0.40	0.24
3(oxidation)	0.42	0.35	0.20
3(reduction)	0.46	0.39	0.22
4(oxidation)	0.41	0.32	0.21
4(reduction)	0.46	0.37	0.23

^a Value obtained using D₂ TPD.

temperatures. The results obtained in this study suggest that the dispersion of supported Rh is not severely damaged by brief high temperature excursions in a H₂-based reducing exhaust when compared Pt/Al₂O₃ catalysts treated in the same way. However, in an oxidizing environment, excursions to high temperature cause rapid oxidation of supported Rh, and subsequent dissolution into the support. With subsequent high temperature treatments in H₂, this Rh is either (1) only partially recovered, or (2) recovered in the form of severely sintered (large) particles. These experiments suggest that the oxidation of these Rh particles can be limited by increasing the cycling frequency during exposure to alternating oxidizing/reducing environments.

Although Rh metal surface area decreases as a result of thermal sintering in each of these environments, the initial effect on the activity of the catalyst may not necessarily be deleterious during the initial stage of sintering (20, 43–47). Although the CO oxidation activity is not expected to be sensitive to the surface structure of the Rh crystallites (44–46), characterization of the CO oxidation activity of these catalysts performed at intervals of the same aging treatments suggest that highly dispersed Rh are less

active than larger Rh particles, as will be discussed in a companion paper.

ACKNOWLEDGMENTS

The authors thank M. J. D'Aniello, Jr., and M. Zammit for chemisorption analysis of the catalyst, and J. Johnson for XRD analysis of some of the aged catalyst samples.

REFERENCES

1. Taylor, K. C., in "Automobile Catalytic Converters." Springer-Verlag, Berlin, 1984.
2. Hughes, R., "Deactivation of Catalysts." Academic Press, London, 1984.
3. Wong, C., and McCabe, R. W., *J. Catal.* **107**, 535 (1987).
4. Martens, J. H. A., Prins, R., and Koningsberger, D. C., *J. Phys. Chem.* **93**, 3179 (1989).
5. Yates, J. T., Jr., Duncan, T. M., Worley, S. D., Vaughan, R. W., *J. Phys. Chem.* **70**, 1219 (1979).
6. Worley, S. D., Rice, C. A., Mattson, G. A., Curtis, C. W., Guin, J. A., Tarrer, A. R., *J. Phys. Chem.* **86**, 2714 (1982).
7. Yang, A. C., and Garland, C. W., *J. Phys. Chem.* **61**, 1504 (1957).
8. Primet, M., *J. Chem. Soc. Faraday Trans 1* **74**, 257 (1978).
9. Cavanagh, R. R., and Yates, J. T., Jr., *J. Chem. Phys.* **74**, 4150 (1981).
10. Paul, D. K., and Yates, J. T., Jr., *J. Phys. Chem.* **95**, 1694 (1991).
11. van't Blik, H. F. J., van Zon, J. B. A. D., Huizinga, T., Vis, J. C., Koningsberger, D. C., and Prins, R., *J. Am. Chem. Soc.* **107**, 3139 (1985).
12. Solymosi, F., and Pasztor, M., *J. Phys. Chem.* **89**, 4789 (1985).
13. Solymosi, F., and Pasztor, M., *J. Phys. Chem.* **90**, 5312 (1986).
14. Basu, P., Panayotov, D., and Yates, J. T., Jr., *J. Phys. Chem.* **91**, 3133 (1987); *J. Am. Chem. Soc.* **110**, 2074 (1988).
15. Zaki, M. I., Kunzmann, G., Gates, B. C., and Knozinger, H., *J. Phys. Chem.* **91**, 1486 (1987).
16. Schwartz, J., and Schmidt, L. D., *J. Catal.* **138**, 283 (1992).
17. Solymosi, F., Bausagi, T., and Novak, E., *J. Catal.* **112**, 183 (1988).
18. Krause, K. R., and Schmidt, L. D., *Catal. Lett.* **14**, 141 (1992).
19. Dictor, R., *J. Phys. Chem.* **93**, 2526 (1989).
20. Fuentes, S., and Figueras, F., *J. Catal.* **61**, 443 (1980).
21. Yates, D. J. C., Murrell, L. L., and Prestridge, E. B., *J. Catal.* **57**, 41 (1979).
22. Yates, D. J. C., and Prestridge, E. B., *J. Catal.* **106**, 549 (1987).
23. Yao, H. C., Japar, S., and Shelef, M., *J. Catal.* **50**, 407 (1977).

24. Beck, D. D., and Carr, C. J., *J. Catal.* **110**, 285 (1988).
25. D'Aniello, Jr., M. J., Monroe, D. R., Carr, C. J., and Krueger, M. H., *J. Catal.* **109**, 407 (1988).
26. Allegheny Ludlum Steel, United States Patent No. 4,414,023, November 8, 1983.
27. Castner, D. C., Sexton, B. A., and Somorjai, G. A., *Surf. Sci.* **71**, 519 (1978).
28. Castner, D. C., and Somorjai, G. A., *Surf. Sci.* **83**, 60 (1979).
29. Yates, J. T., Jr., Thiel, P. A., and Weinberg, W. H., *Surf. Sci.* **84**, 427 (1979).
30. Scolten, J. J. F., Pijpers, A. P., and Hustings, A. M. L., *Catal. Rev.-Sci. Eng.* **27**, 151 (1985).
31. Bertuccio, A., and Bennett, C. O., *Appl. Catal.* **35**, 329 (1987).
32. Kip, B. J., Duivenvoorden, J. B. M., Koningsberger, D. C., and Prins, R., *J. Catal.* **105**, 26 (1987).
33. Wanke, S. E., and Dougharty, N. A., *J. Catal.* **24**, 367 (1972).
34. Cavanagh, R. R., and Yates, J. T., Jr., *J. Catal.* **68**, 22 (1981).
35. Root, T. W., Fisher, G. B., and Schmidt, L. D., *J. Chem. Phys.* **85**, 46, 79 (1986).
36. Richter, J., Gurney, B. A., and Ho, W., *J. Chem. Phys.* **86**, 477 (1987).
37. Peri, J. B., *J. Phys. Chem.* **69**, 211, 220 (1965).
38. Jozwiak, K. W., and Paryjczak, T., *J. Catal.* **79**, 196 (1983).
39. Rasband, P. B., and Hecker, W. C., *J. Catal.* **139**, 551 (1993).
40. Basu, P., Ballinger, T., and Yates, J. T., Jr., *Rev. Sci. Instrum.* **59**, 1321 (1988).
41. Grimm, R. A., Bremer, R. J., and Stonestreet, S. P., SAE Paper No. 800053, *SAE Trans.* **89**, 357 (1980).
42. Sell, J. A., and Chang, M.-F., SAE Paper No. 820388, 1982.
43. Yates, D. J. C., and Sinfelt, J. H., *J. Catal.* **8**, 348 (1967).
44. Duprez, D., Barrault, J., and Geron, C., *Appl. Catal.* **37**, 105 (1988).
45. Del Angel, G. A., Coq, B., Ferrat, G., Figueras, F., and Fuentes, S., *Surf. Sci.* **156**, 943 (1985).
46. Oh, S. H., Fisher, G. B., Carpenter, J. E., and Goodman, D. W., *J. Catal.* **100**, 360 (1986).
47. Peden, C. H. F., Goodman, D. W., Blair, D. S., Berlowitz, P. J., Fisher, G. B., and Oh, S. H., *J. Phys. Chem.* **92**, 1563 (1988).